Published in final edited form as:
Dev Dyn. 2014 July ; 243(7): 917–927. doi:10.1002/dvdy.24133.

Migration of Sea Urchin Primordial Germ Cells

Joseph P. Campanale[1], **Tufan Gökirmak**[1], **Jose A. Espinoza**[1], **Nathalie Oulhen**[2], **Gary M. Wessel**[2], and **Amro Hamdoun**[1,*]

[1]Marine Biology Research Division, Scripps Institution of Oceanography, University of California San Diego, La Jolla, California [2]Department of Molecular Biology, Cell Biology and Biochemistry, Brown University, Providence, Rhode Island

Abstract

Background—Small micromeres are produced at the fifth cleavage of sea urchin development. They express markers of primordial germ cells (PGCs), and are required for the production of gametes. In most animals, PGCs migrate from sites of formation to the somatic gonad. Here, we investigated whether they also exhibit similar migratory behaviors using live-cell imaging of small micromere plasma membranes.

Results—Early in gastrulation, small micromeres transition from non-motile epithelial cells, to motile quasi-mesenchymal cells. Late in gastrulation, at 43 hr post fertilization (HPF), they are embedded in the tip of the archenteron, but remain motile. From 43–49 HPF, they project numerous cortical blebs into the blastocoel, and filopodia that contact ectoderm. By 54 HPF, they begin moving in the plane of the blastoderm, often in a directed fashion, towards the coelomic pouches. Isolated small micromeres also produced blebs and filopodia.

Conclusions—Previous work suggested that passive translocation governs some of the movement of small micromeres during gastrulation. Here we show that small micromeres are motile cells that can traverse the archenteron, change position along the left-right axis, and migrate to coelomic pouches. These motility mechanisms are likely to play an important role in their left-right segregation.

Keywords

small micromere; migration; primordial germ cell; motility; filopodia; cortical bleb; phosphoinositides; live cell imaging

Introduction

Primordial germ cell (PGC) migration from sites of formation to the somatic gonad is essential to development of the germline. Motility and migratory behaviors of PGCs, used to reach the somatic gonad, have been well described in the fly, fish, and mouse (Kunwar et al., 2006; Molyneaux and Wylie, 2004; Richardson and Lehmann, 2010). These studies indicate

*Correspondence to: Amro Hamdoun, 9500 Gilman Drive, La Jolla, CA 92093-0202. hamdoun@ucsd.edu.

that migration of PGCs is characterized by conspicuous dynamics of the migrating PGC plasma membrane, including the extension and retraction of projections such as blebs, filopodia, and lamelli-podia (Raz, 2004). These projections sense PGC position within the embryo and direct their motility towards the forming gonad (Richardson and Lehmann, 2010).

Recent studies in the purple sea urchin, *Strongylocentrotus purpuratus* (*Sp*), indicate that small micromeres are likely to be PGCs, or PGC precursors, because they are required for formation of gametes (Yajima and Wessel, 2011) and express typical germ-line markers (Wessel et al., 2013). Four small micromeres arise at the fifth embryonic cell division, remain quiescent during early development, and divide only once before the end of gastrulation. The eight small micromeres segregate into two separate populations destined for the left and right coelomic pouches of the pluteus larva (Pehrson and Cohen, 1986). Those on the left proliferate and form the larval rudiment, while those in the right undergo apoptosis (Luo and Su, 2012).

Although this left/right segregation is precise, with more than 90% of embryos having a 4/4 or 5/3 pattern (Campanale and Hamdoun, 2012), it has remained unclear whether this process occurs passively by translocation of small micromeres or actively, by migration. A previous study suggested that small micromeres translocate from the vegetal to the animal pole during early gastrulation by the movement of the elongating archenteron (Yajima and Wessel, 2012). Here we investigated whether autonomous small micromere migration could also play a role in their positioning within the embryo.

PGC migration has been extensively studied in *Drosophila melanogaster* (Sano et al., 2005; Santos and Lehmann, 2004; Starz-Gaiano and Lehmann, 2001), *Danio rerio* (Raz, 2003; Tarbashevich and Raz, 2010) and *Mus musculus* (Molyneaux et al., 2001; Stebler et al., 2004). In all three species, migration is mediated by a conserved set of molecular controls (Richardson and Lehmann, 2010; Santos and Lehmann, 2004) that drive stages of motility (Parent and Devreotes, 1999; Ridley et al., 2003; Vicente-Manzanares et al., 2005). These include polarization of membrane receptors (i.e., G protein–coupled receptors), translation of chemotactic cues into focal adhesions, and acto-myosin mediated movements (Lauffenburger and Horwitz, 1996). In migrating cells, these three stages lead to the extension and retraction of the characteristic membrane structures used for sensing and movement. Whether small micromeres also acquire these morphological features of migrating cells is unknown.

Here we used three fluorescent protein fusions, including a PGC-targeted membrane-anchored protein, an apical membrane protein, and a marker of phosphoinostides, to capture membrane dynamics in small micromeres by confocal microscopy. We found that sea urchin small micromeres are motile, actively position at the tip of the archenteron, and can migrate to coelomic pouches. Small micromeres extend and retract numerous cortical blebs and filopodia that appear to orchestrate this motility. Similar membrane dynamics were observed in small micromeres isolated from dissociated gastrulae. Collectively, our results provide a first glimpse into the migration of sea urchin small micromeres.

Results

Small Micromeres Express *nanos2* UTR-Targeted Fluorescent Membrane Markers During Gastrulation

To investigate small micromere membrane morphology during gastrulation, we generated a construct encoding the membrane-anchoring domains of lymphocyte-specific protein tyrosine kinase (LCK) fused to mCitrine fluorescent protein and flanked by the *Sp-nanos2* 3′ and 5′ UTRs. We refer to this construct as *nanos*-targeted membrane mCitrine (NTM-mCit). NTM-mCit accumulated in small micromere membranes, and was significantly enriched in these cells in gastrulae (Fig. 1). Robust NTM-mCit fluorescence was observed in all eight small micromeres at the tip of the archenteron between 43 and 54 hr post fertilization (HPF). At this time, other cells in the embryo had a low background level of NTM-mCit (Fig. 1A–C), but small micromere plasma membranes were always significantly brighter (~2–3 times) than those of any other cell in the embryo.

Expression of NTM-mCit did not disrupt development and morphogenesis of the embryo or the small micromeres. Images showing NTM-mCit overlaid on differential interference contrast (DIC) images of embryos are shown in Figure 1A′–C′. Eggs injected with NTM-mCit mRNA gave rise to healthy gastrulae with normally positioned archenterons at 43 HPF (Fig. 1A′) and progressively elongated skeletons between 49 and 54 HPF (Fig. 1B′–C′). Additionally, the expression of NTM-mCit in the small micromeres did not alter the average 5-left:3-right (Campanale and Hamdoun, 2012; Pehrson and Cohen, 1986) small micromere segregation into the coelomic pouches (Fig. 1D).

Small Micromeres Produce Thin Filopodia and Cortical Blebs Before Segregating to the Left and Right Coelomic Pouches

Since small micromeres transition from a tightly packed cluster to a row of cells that segregate to the coelomic pouches (Fig. 1), we postulated small micromeres move along the tip of the archenteron. In addition, high-resolution confocal snapshots of small micromeres labeled with NTM-mCit indicated small micromeres exhibit morphological features of motile cells (Fig. 2). At 43 HPF, small micromeres were tightly packed at the tip of the archenteron and projected microvilli into the lumen of the archenteron (Fig. 2A). Consistent with this epithelial-like morphology, the small micromeres formed a single layer of cells with adherent lateral membranes (Fig. 2A). However, unlike most epithelial cells in the embryo, small micromeres began to produce filopodia from their blastocoelar/basal membranes that projected toward the animal pole (Fig. 2A,B). Each small micromere developed more than one filopodium, and we often observed multiple filopodia contacting the basal surfaces of cells in the animal pole ectoderm (Fig. 2B). Additionally, small micromeres also produced numerous cortical blebs from the basal membrane (Fig. 2A,B). These blebs ranged from less than 1 μm to several microns in diameter and were exclusively observed extending into the blastocoel from areas of membrane lacking filopodia (Fig. 2B).

By 49 HPF, small micromeres were less tightly packed into the tip of the archenteron (Fig. 2C,D) and were arranged in a line at the top of the archenteron. They extended filopodia contacting the animal pole ectoderm and spread throughout the blastocoel laterally (Fig.

2C). 3D reconstructions of confocal images indicated that small micromeres always extended filopodia that were in contact with apical ectoderm. Small micromeres were found in the dorsal roof of the archenteron after it turned toward oral ectoderm (Fig. 2D). Several non-small micromeres, presumably SMC-derived cells, were also positioned on the roof of the archenteron and extended filopodia that contacted the ectoderm. Membrane blebs were observed in small micromeres, although less frequently than at 43 HPF. Small micromeres typically retained contact with one another and began to form a line along the left/right axis of the archenteron before fusion of endodermal and ectodermal epithelia to form the mouth (Fig. 2C,D).

By 54 HPF, the SMCs began to form the coelomic pouches (Fig. 2E,F) and small micromeres formed a row on the dorsal roof of the archenteron. However, unlike earlier time points, the line of eight cells was sometimes split into two groups, each group nearer a single forming coelomic pouch (Fig. 2E,F). Small micromeres continued to produce long filopodia that contacted the basal side of the animal ectoderm and that spread laterally throughout the blastocoel (Fig. 2E,F). Interestingly, each small micromere extended filopodia towards only one coelomic pouch (Fig. 2F), suggesting that small micromeres use filopodia to discriminate between the coelomic pouches. At 54 HPF, small micromeres produced smaller and less frequent cortical blebs than at 49 HPF.

Small Micromeres Undergo Changes in Apciobasal Polarity During Migration

While previous studies indicated that small micromeres de-epithelialize in early development, we observed that small micromeres were organized as a single layer of cells at the archenteron tip in late gastrulae (Fig. 2) with apparent microvillar projections of into the lumen of the archenteron (Fig. 2A). To investigate the extent to which small micromeres de- and/or re-epithelialized during gastrulation, embryos were labeled with the small micromere marker Vasa-mChr and the membrane protein G2a-mCit, which localizes exclusively to apical membranes of polarized epithelial cells (Gokirmak et al., 2012).

In mesenchyme blastulae (22 HPF), G2a-mCit localized to apical microvilli of all cells in the blastoderm, including the small micromeres (Fig. 3A). G2a-mCit was absent from the primary mesenchymal cells (PMCs) that had ingressed into the blastocoel (Fig. 3A). Similar clearing of G2a-mCit protein could be observed in presumptive mesenchyme cells surrounding the small micromeres, as they removed apical membrane before ingression into the blastocoel (Fig. 3A,B). Initiation of gastrulation occurred at 29 HPF and included the de-epithelialization of small micromeres from the vegetal blastoderm (Fig. 3B). In contrast, ingressing small micromeres did not completely remove G2a-mCit as observed in the PMCs, and G2a-mCit was faintly present around the entire small micromere membrane (Fig. 3B). At 36 HPF, small micromeres were typically found to be in the epithelium and had microvilli (Fig. 3A) and more intense G2a-mCit fluorescence localized around the entire cell (Fig. 3A,B).

Small micromeres appeared re-epithelialized into the blastoderm at the very tip of the archenteron at 43 HPF (Fig. 3B). While G2a-mCit staining was restricted to apical microvilli of endoderm lining the lumen of the archenteron, small micromeres had G2a-mCit protein around the entire cell now highlighting both apical microvilli and lateral membranes (Fig.

3B). As with NTM-mCit, the G2a-mCit revealed that small micromeres were packed at the tip of the archenteron and projected basal blebs and filopodia into the blastocoel (Fig. 3B).

At 49 HPF, G2a-mCit fluorescence was absent from the subset of PMC and SMC lineages that had undergone EMT while the small micromeres, SMCs, and endoderm of the extended archenteron showed G2a-mCit localization lining the lumen of the archenteron (Fig. 3A,B). G2a-mCit continued to be expressed on the entire small micromere plasma membrane through 54 HPF (Fig 3B).

Small Micromeres Move Faster Than Endoderm or SMCs of the Achenteron

Given that the snapshots of small micromeres overexpressing NTM-mCit and G2a-mCit indicated they underwent morphological and positional changes characteristic of migrating cells, we sought to determine whether they were motile. We collected 2-hr time-lapse recordings of fluorescently labeled small micromeres expressing NTM-mCit and mCherry fused *Sp-vasa* (Vasa-mChr) during gastrulation. As with NTM-mCit, expression of Vasa-mChr did not affect the left-right segregation patterns of small micromeres as compared to vasa-immunolocalized controls (Fig. 1D).

Confocal time-lapse recordings showed that small micromeres always moved several microns in the X, Y, and/or Z planes, indicating that they are motile. In contrast, endoderm cells jostled in all three dimensions, but did not displace significantly from their origin (Figs. (4 and 5)). At 43 HPF, small micromeres migrated in the plane of the epithelium while producing filopodial extensions (Fig. 4A; see Supp. Movie S1, which is available online). A subset of small micromeres made striking migratory movements around the archenteron. For example, Supp. Movie S1 shows a small micromere moving past a neighboring small micromere before coming to rest on the other side of the archenteron. These “neighbor switching” movements indicated that small micromeres oriented along the left/right axis as they jostle for position. Depending on the original orientation of the embryo being time-lapsed, small micromeres translocated to the roof of the archenteron as it turned toward the stomodeum.

At 49 HPF, small micromeres moved laterally and positioned themselves along the left/right axis (Fig. 4B, Supp. Movie S2). While all small micromeres moved, a few had especially long tracks, often traversing the entire length of the archenteron tip. After the small micromeres formed a line along the left/right axis on the dorsal surface of the archenteron, they moved in the direction of the closest coelomic pouches (Fig. 4C, Supp. Movie S3).

Small micromere motility often produced net movement in a single direction, whereas motility of other cell types was more random. To measure movements of different cell types we compared small micromere track statistics to those of both SMC cells (that are incorporated into the coelomic pouches) and endodermal cells on the archenteron. All cell types tracked moved/jostled in all three dimensions (Fig. 5A,B, Supp. Movies S4, S5, S6); however, this motility only led to net movement in small micromeres and SMCs. We refer to this net movement from origin as “displacement.”

In 43-hr-old gastrulae, small micromeres displaced farther from their origin and moved at greater velocities than either SMCs or endoderm cells (Fig. 5C,D). On average, small micromeres displaced 4.64 (±0.61 s.e.m.) μm from their origin, while SMC and archenteron cells displaced only 2.37 (±0.40) and 2.05 (±0.35) μm, respectively (Fig. 5C,D). Small micromere velocity was 13.28 (±0.78) μm/hr, while SMCs and endoderm cells moved at lower velocities of 8.77 (±0.66) and 6.14 (±0.79) μm/hr, respectively.

Similarly, small micromeres also tracked farther and faster than other cells at 49 and 54 HPF (Fig. 5C,D). Between 49 and 54 HPF, small micromeres maintained a significantly higher velocity at roughly 13 μm/hr, while SMCs maintained velocities nearing 9 μm/h, and endoderm cells moved less than 5.5 μm/hr (Fig. 5D). Beginning at 49 HPF, the displacement of the presumptive coelomic pouch SMCs became statistically indistinguishable from the small micromeres at 3.53 (±0.40) and 4.67 (±0.80) μm, respectively (Fig. 5C). These values slightly decreased at 54 HPF to 3.03 (±0.51) and 3.96 (±0.46) μm, respectively (Fig. 5C). Both the SMC and the small micromere lineages showed highly variable displacements (Fig. 5D). These results potentially reflect the fact that SMCs and small micromeres in the middle of the archenteron must move a greater distance to reach the left or right coelomic pouches than those that start closer to the pouches.

Enhanced Expression of the PIP_2 Binding PH-Domain From PLC-Delta in Small Micromeres

Phosphatidylinositol 3-kinase (PI3K) is required for the migration of numerous cell types (Cain and Ridley, 2012). PI3K phosphorylates phosphatidylinositol 4,5-bisphosphate (PrP_2) at the leading edge of migrating cells into phosphatidylinositol 3,4,5-triphos-phate (PIP_3; Huang et al., 2003). To observe the distribution of phosphoinositides in small micromeres, we localized PIP_2 by co-injecting mRNA encoding the pleckstrin homology domain of phospholipase C-delta (PH^{PLC}-delta) fused to mCitrine (PH-mCit) along with mRNA encoding Vasa-mChr. PH-mCit localized to cellular membranes of all cells in the embryo, and was brighter in small micromeres than all other cells (Fig. 6).

Small micromeres over-expressing PH-mCit underwent normal morphogenesis and segregated to the coelomic pouches (Fig. 6, Supp. Movie S7). At 43 HPF, small micromeres produced characteristic blebs that extended into the blastocoel (Fig. 6A,B). After left/right archenteron positioning, small micromeres produced several filopodia that extended into the blastocoel and contacted the basal membranes of ectoderm cells (Fig. 6C–G). Figure 6H (Supp. Movie S7) shows the track from a single small micromere located in the middle of the archenteron that used filopodia to contact the ectoderm before migrating to the anterior tip of a forming coelomic pouch while producing a combination of blebs and filopodia (Fig. 6).

There are at least two types of filopodia in motile mesenchymal cells of sea urchin embryos (Miller et al., 1995). Thin filopodia, which are different from thick migratory filopodia, are produced in SMCs at the tip of the archenteron and have variable ectodermal contacts and retraction dynamics. The proposed function of the thin filopodia in SMCs are for the detection of bound chemical signals on the basal lamina of ectoderm, rather than the detection of diffusible morphogens (Miller et al., 1995). Small micromeres extended thin

filopodia that robustly retained fluorescent PH-mCit staining at the same time when SMCs at the tip of the archenteron use these structures to find the future stomodeum (mouth opening, Fig. 6). Therefore we sought to observe filopodial behavior in small micromeres expressing PH-mCit using timelapse confocal microscopy.

After the small micromeres had migrated to the coelomic pouches at 60 HPF, they produced two types of filopodia, short-lived and long-lived. Short-lived filopodia extended from small micromeres that lasted only a few minutes (Fig. 7B). Often these filopodia extended into the blastocoel and did not make contact with the ectoderm. We also observed a subset of long-lived filopodia that consistently contacted the ectoderm for periods of greater than 45 min (Fig. 7A). Interestingly, Supp. Movie S7 showed small micromeres produce filopodia that were not always oriented in the direction of movement. These results (Fig. 6, Supp. Movie S7) suggest that small micromeres, like the SMCs, might use thin filopodia to detect extracellular substances or position while blebs generate motility.

Small Micromeres Maintain Migratory Cell Morphology and Behavior In Vitro

We observed that small micromeres, like the PGCs of zebrafish, produce large cortical blebs at the onset of migration (Fig. 2). In zebrafish, these short-lived blebs are extended and retracted rapidly to propel large portions of the cell body in a single direction (Blaser et al., 2006). Since small micromeres also produced these cortical blebs (Figs. (1 and 2)), we analyzed the behavior of blebs *in vivo*, using confocal time-lapse recordings of small micromeres expressing NTM-mCit. Small micromere cortical blebs were highly dynamic, expanding and contracting in less than one minute (Fig. 8A, Supp. Movies S8, S9).

To further investigate these blebs, we performed confocal time-lapse recordings of individual small micromeres from embryos dissociated at 43 and 49 HPF. After dissociation, small micromeres continued to produce and retract blebs within seconds. They also projected filopodia that expanded and contracted at rates similar to those observed in vivo (Fig. 8B, Supp. Movies S10, S11). These results are consistent with bleb dynamics for other migratory PGCs (Blaser et al., 2005) and are distinct from the persistent blebs of apoptotic cells (Taylor et al., 2008).

Discussion

Using live cell imaging, we observed at least three phases of small micromere movement from the tip of the archenteron to the coelomic pouches (Fig. 9). The start of their movements to the coelomic pouches begins from a re-epithelialized group of cells on the tip of the archenteron that produce cortical blebs. Next, small micromeres extend filopodia and position in a line along the left/right axis. Finally, the filopodia are projected laterally into the blastocoel while small micromeres move towards the forming coelomic pouches (Figs. (1 and 5), 9).

Of the three archenteron cell types that we tracked, small micromeres moved at the highest average velocity, while presumptive coelomic pouch SMCs and endodermal cells of the archenteron moved at much lower velocities. Small micromere motility was initiated late in gastrulation, a similar developmental stage to which PGCs become motile in *Danio* and

Drosophila. Sea urchin small micromeres moved at a rate of ~13 μm/hr, comparable to that of mouse PGCs at 10 μm/hr (Molyneaux et al., 2001), but slower than PGCs of *Drosophila* and *Danio*, which move at 54 and 120 μm/hr, respectively (Reichman-Fried et al., 2004; Sano et al., 2005).

While the tracks of sea urchin PGCs were sometimes more directed than the tracks of the other cells measured (Figs. 4A, 5A,B), we observed significant variation in the direction of motility between individual small micromeres. For example, in the same embryo we observed one small micromere contacting oral ectoderm with filopodia and moving 10–20 μm away from its origin (Fig. 6; Supp. Movie S7), while several of its neighboring small micromeres did not appear to move away from their starting position. This may simply indicate that small micromeres do not move collectively to the coelomic pouch, and will continue to jostle individually towards the posterior end of the coelomic pouch (Luo and Su, 2012).

Alternatively, given that some small micromeres are closer to the developing coelomic pouches than others, one possibility is that the distance migrated by a small micromere is influenced by the distance to be traveled to a coelomic pouch. Consistent with this hypothesis, the highly motile small micromere in this experiment was positioned in the middle of the archenteron and had the greatest distance to travel. Thus, sea urchin small micromeres could be similar to other PGCs in that they are motile during gastrulation, but unique from other organisms in that they use this motility as a “quality control” mechanism to either maintain an existing position or to displace/translocate towards an alternate position.

PIP signaling is characteristic of migrating cells (Cain and Ridley, 2012) and we observed that small micromeres had an enhanced expression of the PH-mCit. The enhanced expression of PH-mCit could reflect a concentration of PIP_2 in their plasma membrane, which would concentrate the fluorescent signal (Thaler et al., 2004). We also considered that the exogenous protein could be expressed at higher concentrations in small micromeres because they can retain exogenous mRNAs (Oulhen and Wessel, 2013). However, retained mRNA appears to require globin UTRs, which were absent from our construct. Therefore, retention does not seem to be the most likely explanation. Indeed, consistent with this expectation, several of our other membrane proteins and nuclear markers (that lack globin UTRs) are not enriched in small micromeres of blastulae (Gokirmak et al., 2012). Thus, the enrichment seems most likely to be a function of the interaction between PH-mCit with phosphoinositides in small micromere membranes.

It was previously noted that the translocation of small micromeres in early gastrulation is passive and requires their adhesion to one another with G-cadherin (Yajima and Wessel, 2012). Here, we observe a transition beginning late in gastrulation at 43–49 HPF when the cells move from a tightly packed ball of cells to a loosely associated single line, potentially indicating the onset of their motility along the left/right axis. Consistent with this hypothesis, small micromeres isolated from embryos at 43 and 48 HPF also bleb and extend filopodia. Remarkably, when small micromeres are isolated from the embryo much earlier in development and cultured with their sister cell lineage, the primary mesenchymal cells, they

autonomously express germline genes, including *vasa* and *nanos*, yet did not activate a migratory program or produce cortical blebs (Yajima and Wessel, 2012). These results might indicate that the initiation of small micromere motility requires initial contact with neighboring cells or secreted signals but that it is self-maintaining once initiated.

Cadherins are important for maintaining cell–cell contacts as well as for PGC migration (Kardash et al. 2009). G-cadherin is expressed at high levels in small micromeres (Miller and McClay, 1997). Morpholino knockdown of G-cadherin causes small micromeres to either trans-differentiate into PMCs or die (Yajima and Wessel, 2012). G-cadherin might be required for small micromeres to re-join the blastoderm before they migrate. Using the membrane marker, NTM-mCit, and the apical marker G2a-mCit, we found that small micromeres always retained contact with the lumen of the archenteron and usually had microvilli, a characteristic of epithelial cells. In contrast, endoderm cells express G2a-mCit only on their apical surface while mesenchymal PMCs do not retain any G2a-mCit expression. However, small micromeres did not restrict G2a-mCit to only the archenteron luminal/apical membrane, and also had some features of mesenchymal cells.

One function of small micromere migration could be the segregation of the appropriate number of small micromeres to the left and right coelomic pouches. Consistent with this hypothesis, small micromeres segregate to left and right coelomic pouches precisely (Campanale and Hamdoun, 2012; Pehrson and Cohen, 1986; Tanaka and Dan, 1990). The mechanisms that govern this ordered segregation remain unclear but it seems likely that the autonomous motility we report is important. It was previously demonstrated that segregation is disrupted by inhibiting ABC transporter activity (Campanale and Hamdoun, 2012), or disrupting Nodal signaling (Luo and Su, 2012), suggesting that small micromeres migrate to the coelomic pouches using signals that specify the left/right axis. Further studies into this migration could provide insight into the mechanisms by which motility is regulated along the left-right axis.

Experimental Procedures

Animal Collection, Egg Microinjection, and Embryo Culture

Adult *Strongylocentrotus purpuratus* were collected in La Jolla, CA, and held at 11°C (± 1°C) in flow-through seawater aquaria. Spawning and gamete gathering was performed as described previously (Campanale and Hamdoun, 2012). For microinjection, eggs were held on protamine sulfate coated delta-T dishes (Bio-ptechs, Butler, PA), and mRNA was injected at 2–5% of egg volume (Lepage and Gache, 2004). Injected embryos were cultured in filtered seawater (FSW) containing 100 μg/ml ampicillin (Sigma, St Louis, MO) at 15°C (± 0.5°C) for 24 hr, then plucked and cultured to gastrula stage in FSW lacking ampicillin.

Constructs Targeting Fluorescent Proteins to Small Micromeres

Small micromere membranes were visualized using exogenous expression of fluorescent proteins fused to a membrane- anchoring domain, a pleckstrin homology domain (PH-domain) of phospholipase C-delta, or the ABC transporter, ABCG2a. An open reading frame (ORF) encoding two tandem membrane anchoring domains of lymphocyte tyrosine

kinase (LCK) fused to mCitrine fluorescent protein was cloned into a modified pGEM-T expression vector containing the *Sp-nanos2* 5′ and 3′ untranslated regions (UTRs) (Oulhen et al., 2013). This construct created a nanos-targeted membrane mCitrine (NTM-mCitit). The sequence encoding the PH-domain of Phospholipase C Delta (PH^{PLC}-domain (Stauffer et al., 1998) was inserted downstream of a mCitrine sequence into the pCS2+8 expression vector (PH-mCit, Gokirmak et al., 2012). ABCG2a was fused to mCitrine using the pCS2+8 vector (G2a-mCit, Gokirmak et al., 2012). mCherry fused Sp-vasa was previously described (Vasa-mChr, Campanale and Hamdoun, 2012). Capped mRNAs for all constructs were synthesized in vitro from cDNA templates in either the pGEM-T or pCS2+8 vectors using a T7 Ultra or a SP6 mMessage mMachine kit (Ambion Inc., Austin, TX). Small micromere morphology was observed after micro-injection of 150 ng/μl mRNA encoding NTM-mCitit, or by co-injection of 250 ng/μl each of mRNA encoding Vasa-mChr and PH-mCit or with 1,000 ng/μl G2a-mCit.

Imaging of Small Micromere Morphology and Motility

Embryos were attached to protamine-coated coverslips and visualized using a 40× water immersion objective (numerical aperture of 1.1) on either a Zeiss LSM 700 confocal microscope (Jena, Germany), or a Leica SP-8 confocal microscope (Wetzlar, Germany). Time-lapse recordings of cell migration were performed by immobilizing embryos between two protamine coated coverslips at 15°C and capturing ~24 × 2.5 μm z-slices at 5-min intervals for 1–4 hr. Cell velocity, displacement from origin, and track distance were measured in at least three embryos at each time-point and compared to at least four secondary mesenchyme cells (SMCs) and four non-motile archenteron cells per embryo using the mTrackJ plugin (Meijering et al., 2012) in ImageJ. Briefly, we used Vasa-mChr fluorescence to identify the equatorial position of individual nuclei and measured the change in coordinate positions between each time-point along the X, Y, and Z-axes. Background expression of Vasa-mChr in all cells of the embryo allowed us to track cells in the archenteron and the SMC lineage. The first hour of time-lapse data was quantified to measure the velocity and displacement. To compare the migratory behaviors of the small micromeres to SMC and archenteron cells, we normalized the X, Y, Z coordinates of all cells tracked from individual embryos so that all cells started from the origin, (0,0,0).

Embryo Dissociation and In Vitro Small Micromere Morphology

At specific hours post fertilization (HPF), roughly 250 embryos expressing NTM-mCit and Vasa-mChr were washed with hyalin extraction medium and calcium-magnesium free seawater (McClay and Fink, 1982) for 1 min each, dissociated by shearing through a pipette and washed once with FSW. Cells were settled on protamine-coated coverslips for 5 min. Small micromeres were identified by their enhanced expression of Vasa-mChr and NTM-mCit. A 2.2-μm-thick equatorial section was imaged on a Leica SP8 confocal microscope at 5-sec intervals with a 40 × water immersion objective.

Statistics

All statistics were analyzed using JMP 10.0 (Cary, NC). In all cases an ANOVA ($\alpha \leq 0.05$) with Tukey-Kramer post-hoc multiple comparisons was used to analyze statistical

differences between cell types among embryos from multiple females. The number of batches and embryos used for each experiment are given in each figure legend.

Supplementary Material

Refer to Web version on PubMed Central for supplementary material.

Acknowledgments

We thank P. Zerofski for collecting sea urchins. We thank L. E. Shipp, V. D. Vacquier, and N.D. Holland for discussion of the research and G. W. Moy, R. Z. Hill, L. Mesrop, and S. C. T. Nicklisch for review of the manuscript. J.P.C. and A.H designed the research, J.P.C., T.G., J.A.E. performed the research, J.P.C., T.G., N.O., and G.M.W. contributed new reagents, J.P.C., J.A.E., and A.H. analyzed data, and J.P.C., A.H. wrote the article. This work was supported by a United States Environmental Protection Agency (EPA) STAR Fellowship (FP-91711601-0 to J.P.C. and NIH training grant 5t32gm067550) and by the National Institutes of Health (HD058070 to A.H. and 2R01HD028152 to G.M.W.).

References

Blaser H, Eisenbeiss S, Neumann M, Reichman-Fried M, Thisse B, Thisse C, Raz E. Transition from non-motile behaviour to directed migration during early PGC development in zebrafish. J Cell Sci. 2005; 118:4027–4038. [PubMed: 16129886]

Blaser H, Reichman-Fried M, Castanon I, Dumstrei K, Marlow FL, Kawakami K, Solnica-Krezel L, Heisenberg C-P, Raz E. Migration of zebrafish primordial germ cells: a role for myosin contraction and cytoplasmic flow. Dev Cell. 2006; 11:613–627. [PubMed: 17084355]

Cain RJ, Ridley AJ. Phosphoinositide 3-kinases in cell migration. Biol Cell. 2012; 101:13–29. [PubMed: 19055486]

Campanale JP, Hamdoun A. Programmed reduction of ABC transporter activity in sea urchin germline progenitors. Development. 2012; 139:783–792. [PubMed: 22274698]

Gokirmak T, Campanale JP, Shipp LE, Moy GW, Tao H, Hamdoun A. Localization and substrate selectivity of sea urchin multidrug (MDR) efflux transporters. J Biol Chem. 2012; 52:43876–43883. [PubMed: 23124201]

Huang YE, lijima M, Parent CA, Funamoto S, Firtel RA, Devreotes P. Receptor-mediated regulation of PI3Ks confines PI(3,4,5)P3 to the leading edge of chemotaxing cells. Mol Biol Cell. 2003; 14:1913–1922. [PubMed: 12802064]

Kardash E, Reichman-Fried M, Maître J-L, Boldajipour B, Papusheva E, Messerschmidt E-M, Heisenberg C-P, Raz E. A role for Rho GTPases and cell-cell adhesion in single-cell motility in vivo. Nat Cell Biol. 2009; 12:47–53. [PubMed: 20010816]

Kunwar PS, Siekhaus DE, Lehmann R. In vivo migration: a germ cell perspective. Annu Rev Cell Dev Biol. 2006; 22:237–265. [PubMed: 16774460]

Lauffenburger DA, Horwitz AF. Cell migration: a physically integrated molecular process. Cell. 1996; 84:359–369. [PubMed: 8608589]

Lepage T, Gache C. Expression of exogenous mRNAs to study gene function in the sea urchin embryo. Methods Cell Biol. 2004; 74:677–697. [PubMed: 15575626]

Luo Y-J, Su Y-H. Opposing nodal and BMP signals regulate left-right asymmetry in the sea urchin larva. PLOS Biol. 2012; 10:e1001402. [PubMed: 23055827]

McClay DR, Fink RD. Sea urchin hyalin: appearance and function in development. Dev Biol. 1982; 92:285–293. [PubMed: 6180943]

Meijering E, Dzyubachyk O, Smal I. Methods for cell and particle tracking. Methods Enzymol. 2012; 504:183–200. [PubMed: 22264535]

Miller J, Fraser SE, McClay D. Dynamics of thin filopodia during sea urchin gastrulation. Development. 1995; 121:2501–2511. [PubMed: 7671814]

Miller JR, McClay DR. Characterization of the role of cadherin in regulating cell adhesion during sea urchin development. Dev Biol. 1997; 192:323–339. [PubMed: 9441671]

Molyneaux K, Wylie C. Primordial germ cell migration. Int J Dev Biol. 2004; 48:537–544. [PubMed: 15349828]

Molyneaux KA, Stallock J, Schaible K, Wylie C. Time-lapse analysis of living mouse germ cell migration. Dev Biol. 2001; 240:488–498. [PubMed: 11784078]

Oulhen N, Wessel GM. Retention of exogenous mRNAs selectively in the germ cells of the sea urchin requires only a 5”-cap and a 3-”UTR. Mol Rep Dev. 2013; 80:561–569.

Oulhen N, Yoshida T, Yajima M, Song JL, Sakuma T, Sakamoto N, Yamamoto T, Wessel GM. The 3′UTR of nanos2 directs enrichment in the germ cell lineage of the sea urchin. Dev Biol. 2013; 377:275–283. [PubMed: 23357540]

Parent CA, Devreotes PN. A cell’s sense of direction. Science. 1999; 284:765–770. [PubMed: 10221901]

Pehrson JR, Cohen LH. The fate of the small micromeres in sea urchin development. Dev Biol. 1986; 113:522–526. [PubMed: 3512335]

Raz E. Primordial germ-cell development: the zebrafish perspective. Nat Rev Genet. 2003; 4:690–700. [PubMed: 12951570]

Raz E. Guidance of primordial germ cell migration. Curr Opin Cell Biol. 2004; 16:169–173. [PubMed: 15196560]

Reichman-Fried M, Minina S, Raz E. Autonomous modes of behavior in primordial germ cell migration. Dev Cell. 2004; 6:589–596. [PubMed: 15068797]

Richardson BE, Lehmann R. Mechanisms guiding primordial germ cell migration: strategies from different organisms. Nat Rev Mol Cell Biol. 2010; 11:37–49. [PubMed: 20027186]

Ridley A, Schwartz M, Burridge K, Firtel R, Ginsberg M, Borisy G, Parsons J, Horwitz A. Cell migration: integrating signals from front to back. Science. 2003; 302:1704–1709. [PubMed: 14657486]

Sano H, Renault AD, Lehmann R. Control of lateral migration and germ cell elimination by the Drosophila melanogaster lipid phosphate phosphatases Wunen and Wunen 2. J Cell Biol. 2005; 171:675–683. [PubMed: 16301333]

Santos AC, Lehmann R. Germ cell specification and migration in *Drosophila* and beyond. Curr Biol. 2004; 14:R578–R589. [PubMed: 15268881]

Starz-Gaiano M, Lehmann R. Moving towards the next generation. Mech Dev. 2001; 105:5–18. [PubMed: 11429277]

Stauffer TP, Ahn S, Meyer T. Receptor-induced transient reduction in plasma membrane Ptdlns(4,5)P2 concentration monitored in living cells. Curr Biol. 1998; 8:343–346. [PubMed: 9512420]

Stebler J, Spieler D, Slanchev K, Molyneaux KA, Richter U, Cojocaru V, Tarabykin V, Wylie C, Kessel M, Raz E. Primordial germ cell migration in the chick and mouse embryo: the role of the chemokine SDF-1/CXCL12. Dev Biol. 2004; 272:351–361. [PubMed: 15282153]

Tanaka S, Dan K. Study of the lineage and cell cycle of small micromeres in embryos of the sea urchin, *Hemicentrotus pul cherrimus* . Dev Growth Differ. 1990; 32:145–156.

Tarbashevich K, Raz E. The nuts and bolts of germ-cell migration. Curr Opin Cell Biol. 2010; 22:715–721. [PubMed: 20947321]

Taylor RC, Cullen SP, Martin SJ. Apoptosis: controlled demolition at the cellular level. Nat Rev Mol Cell Bio. 2008; 9:231–241. [PubMed: 18073771]

Thaler CD, Kuo RC, Patton C, Preston CM, Yahisawa H, Epel D. Phosphoinositide metabolism at fertilization of sea urchin eggs measured with a GFP-probe. Dev Growth Differ. 2004; 46:413–423. [PubMed: 15606487]

Vicente-Manzanares M, Webb DJ, Horwitz AR. Cell migration at a glance. J Cell Sci. 2005; 118:4917–4919. [PubMed: 16254237]

Wessel GM, Brayboy L, Fresques T, Gustafson EA, Oulhen N, Ramos I, Reich A, Swartz SZ, Yajima M, Zazueta V. The biology of the germ line in echinoderms. Mol Rep Dev n/a–n/a. 2013

Yajima M, Wessel GM. Small micromeres contribute to the germline in the sea urchin. Development. 2011; 138:237–243. [PubMed: 21177341]

Yajima M, Wessel GM. Autonomy in specification of primordial germ cells and their passive translocation in the sea urchin. Development. 2012; 139:3786–3794. [PubMed: 22991443]

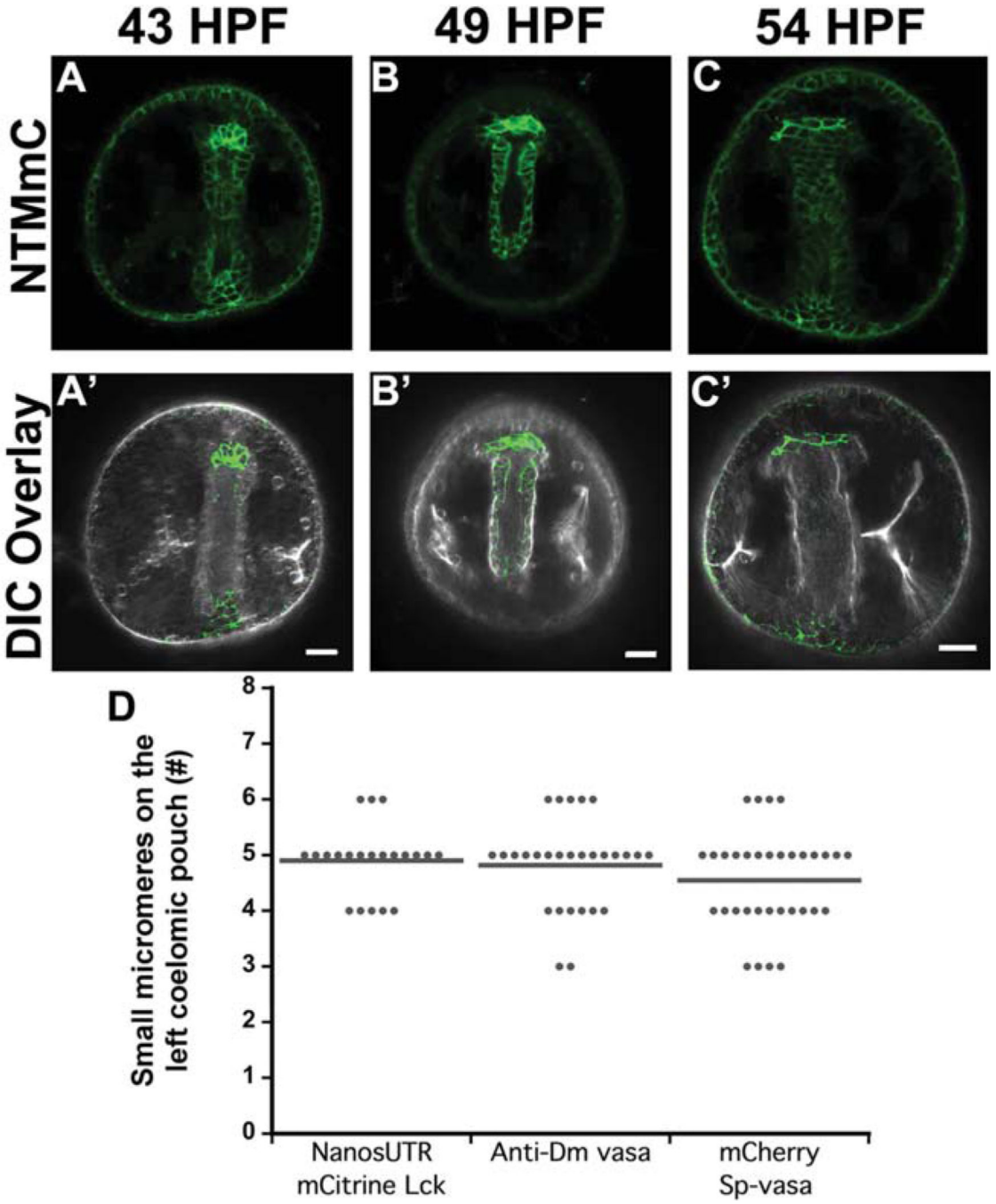

Fig. 1.

Small micromeres expressing NTM-mCit move from the tip of the archenteron to the two coelomic pouches between 43 and 54 HPF. Maximum intensity projections of embryos injected with mRNA encoding NTM-mCit (green) shows small micromeres transition from (**A, A′**) tightly packed cells at 43 HPF to (**B, B′**) a line of cells on the tip of the archenteron at 49 HPF that (**C, C′**) begin segregating among the coelomic pouches at 54 HPF. Top panel, confocal snapshots of fluorescent channel (A–C) and DIC overlay with contrast enhanced fluorescent channel (A′–C′) in bottom panel. Scale bars = 20 μm. **D**: Number of

small micromeres on the left coelomic pouch after overexpression of NTM-mCit, Vasa-mChr or after detection by immunolocalization. N>20 embryos from three females ($P \geq 0.05$, One-way ANOVA).

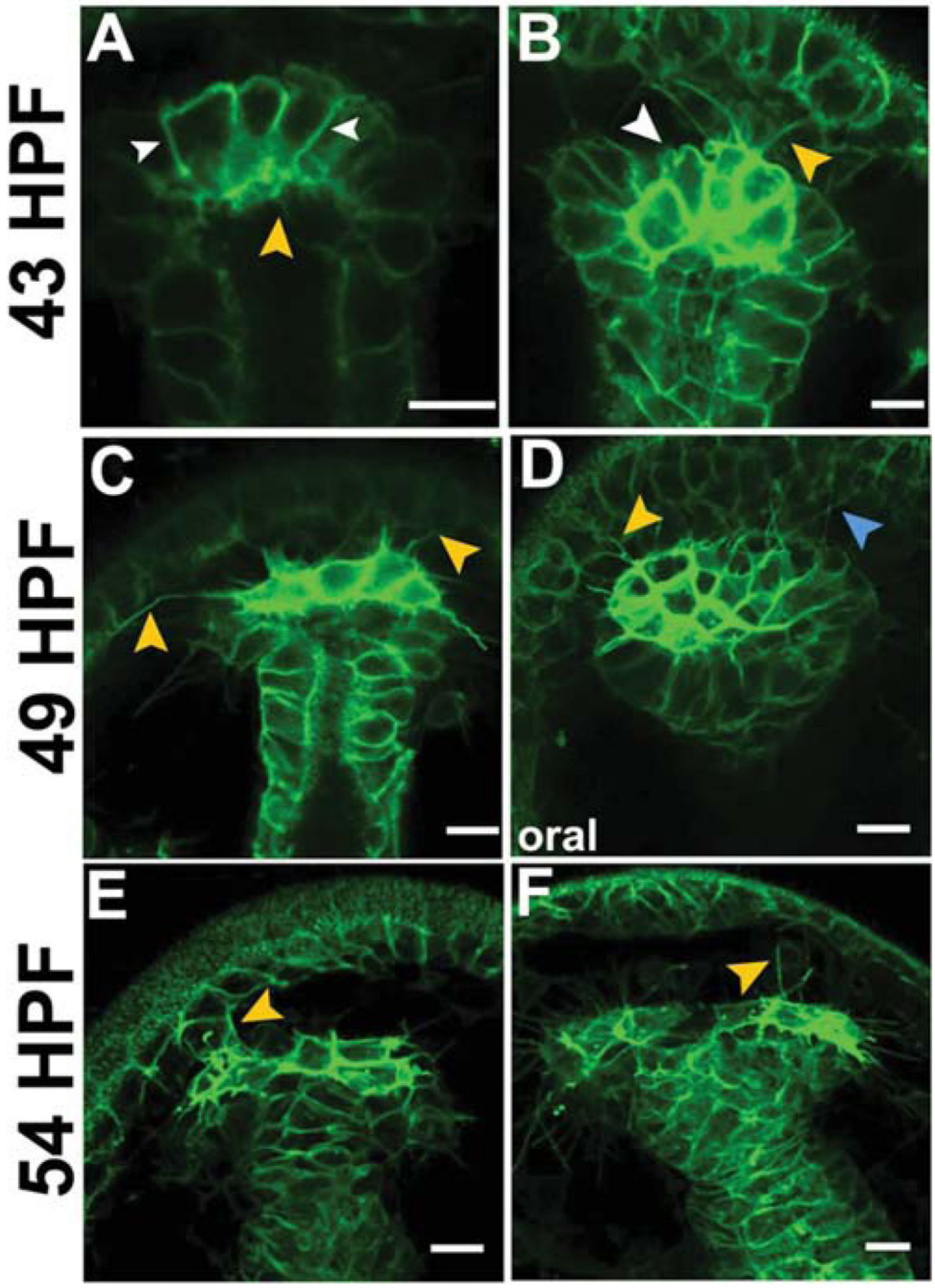

Fig. 2.

Small micromeres develop cortical blebs and thin filopodia before segregating to the coelomic pouches. Representative confocal sections of embryos with small micromeres expressing NTM-mCit (green) with cortical blebs (white arrowheads) at (**A,B**) 43 HPF microvilli or thin filopodia from small micromeres (orange arrowheads) and SMCs (blue arrowhead) contacting ectoderm at (**C,D**) 49 HPF and (**E,F**) 54 HPF. Scale bars = 10 μm.

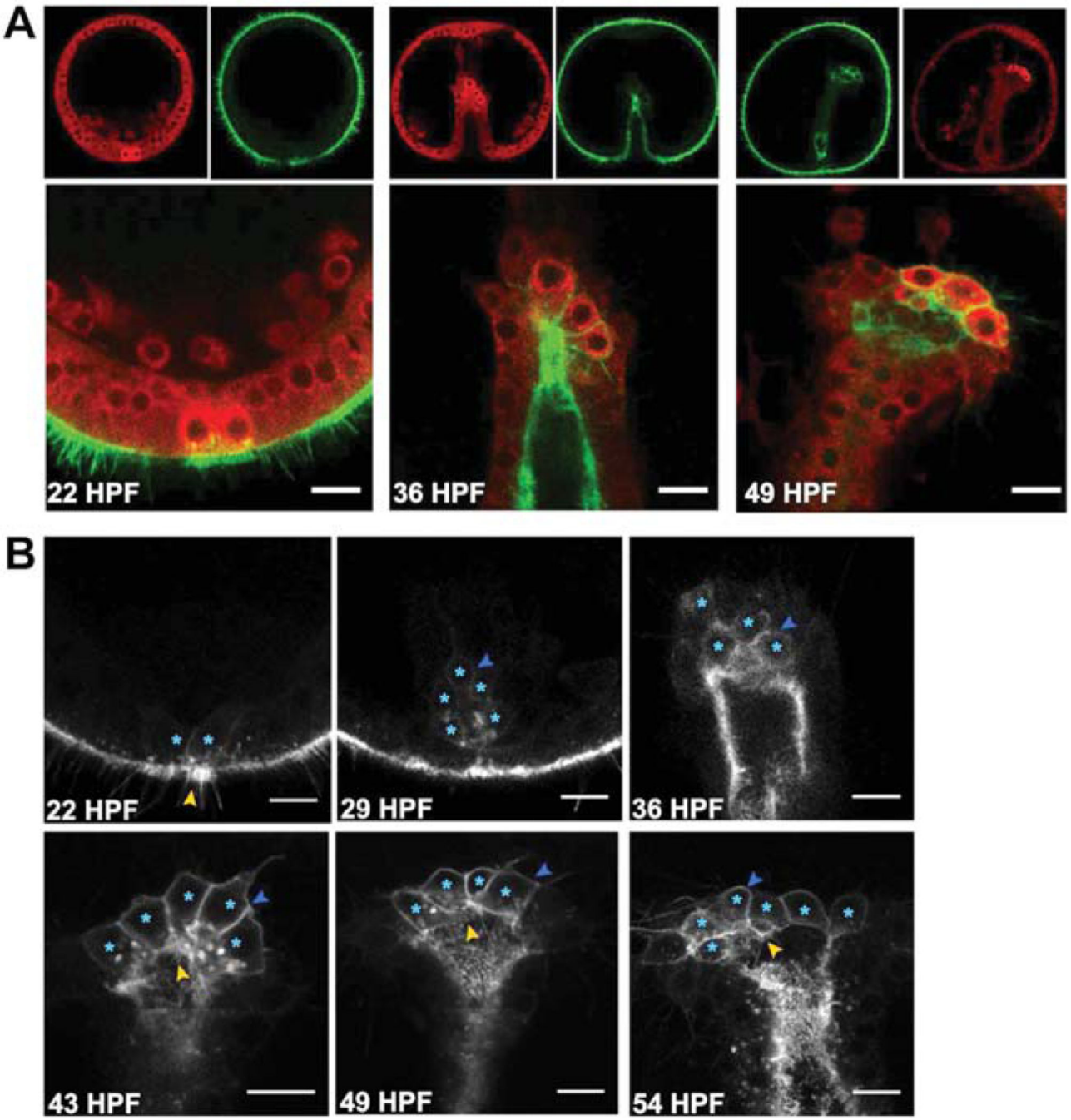

Fig. 3.

Localization of the apical marker G2a-mCit. Representative confocal images of embryos expressing Vasa-mChr (red) and G2a-mCit (green or gray). Symbols indicate small micromeres (blue asterisks), microvilli (orange arrowheads), lateral membrane (blue arrowheads). **A:** Whole embryo fluorescence of Vasa-mChr and G2a-mCit accompanied by an overlay at regions with small micromeres for mesenchyme blastula at 22 HPF, mid-gastrula at 36 HPF, and late gastrula at 49 HPF. **B:** G2a-mCit in small micromeres of the

mesenchyme blastula at 22 HPF, early gastrula at 29 HPF, mid-gastrula at 29 HPF, full gastrula at 43–54 HPF. All scale bars = 10 μm.

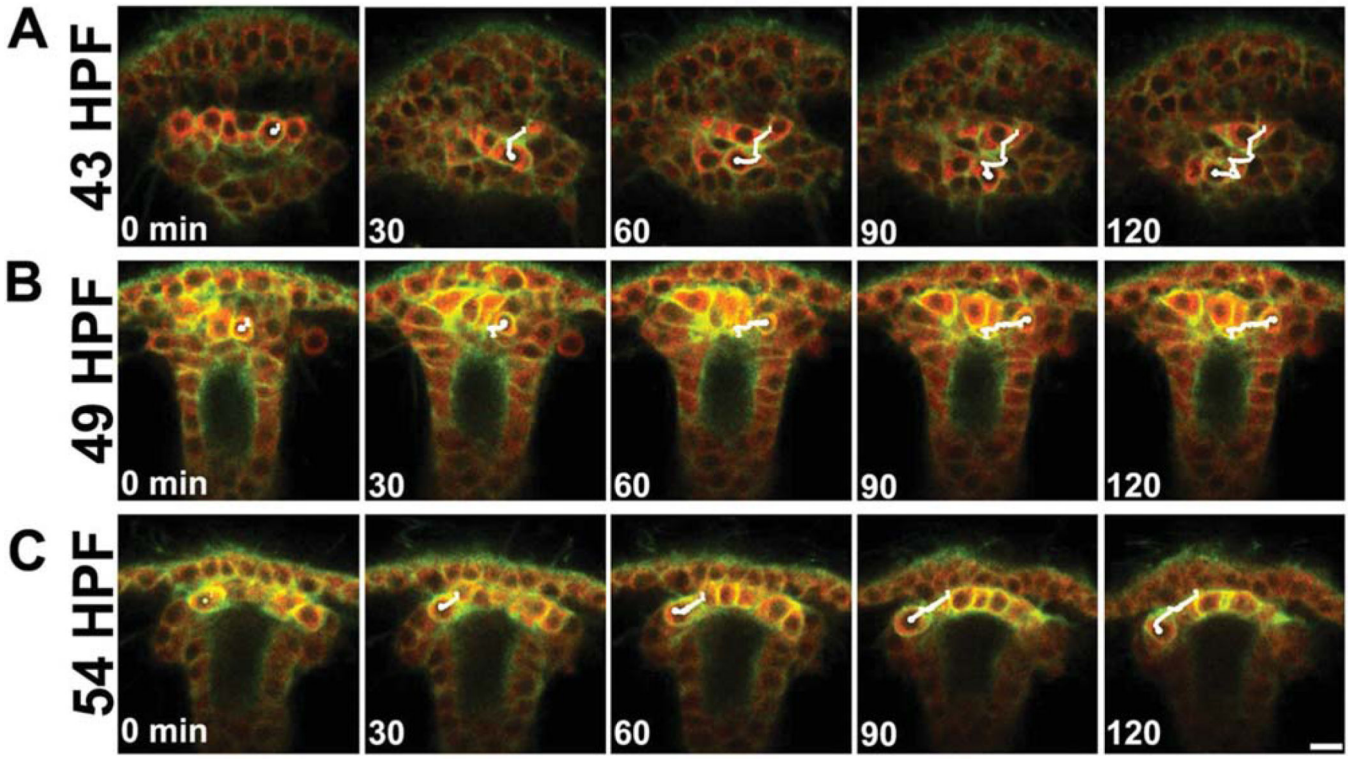

Fig. 4.

Small micromeres move through the tip of the archenteron between 43 and 54 HPF. Embryos expressing NTM-mCit (green) and Vasa-mChr (red) were time lapsed for 120 min by confocal microscopy and tracked (white lines) using mTrackJ. Representative tracks show (**A**) small micromeres moved around the tip of the archenteron before (**B**) moving to form a line at the tip of the archenteron and (**C**) segregating among the left and right coelomic pouches. Scale bar = 10 μm.

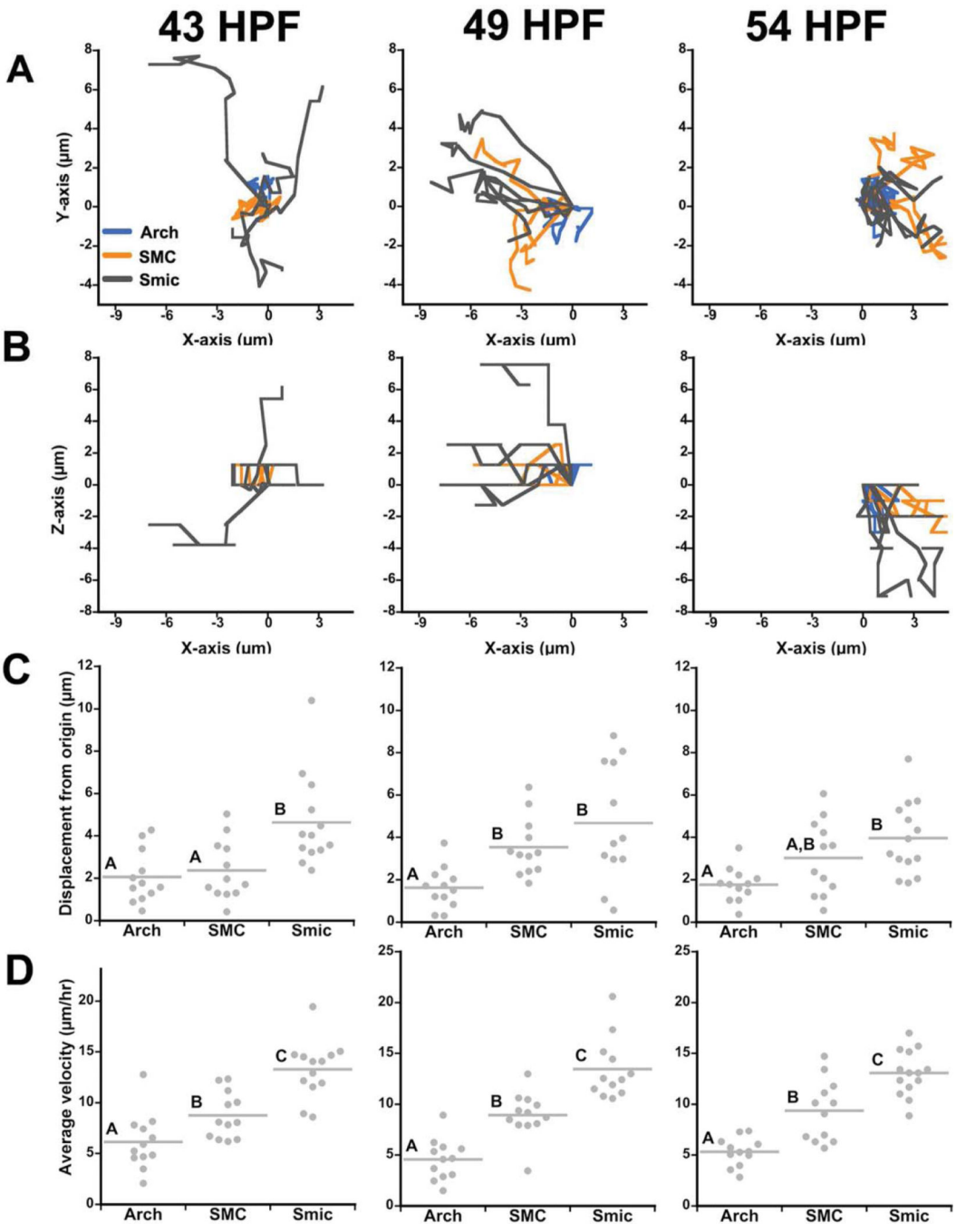

Fig. 5.

Small micromeres move farther and faster than endoderm or SMCs that produce the coelomic pouch. Line plots display representative tracks of the micrometers traveled over 1 hr in the (**A**) x–y direction and (**B**) x–z direction of four small micromeres, SMCs, and endoderm cells between 43 and 54 HPF. Each track was normalized and plotted from a common origin (0,0). Dot plots of (**C**) total displacement from origin and (**D**) average cell velocity for all small micromeres, SMCs, and endoderm cells measured after 1 hr. Each dot represents the micrometers traveled from the origin or the average velocity of one cell and

the bar represents the mean of at least four cells of each type measured from three different embryos (n≥12 cells). Letters above mean lines denote statistical significance ($P \leq 0.05$, two-way ANOVA).

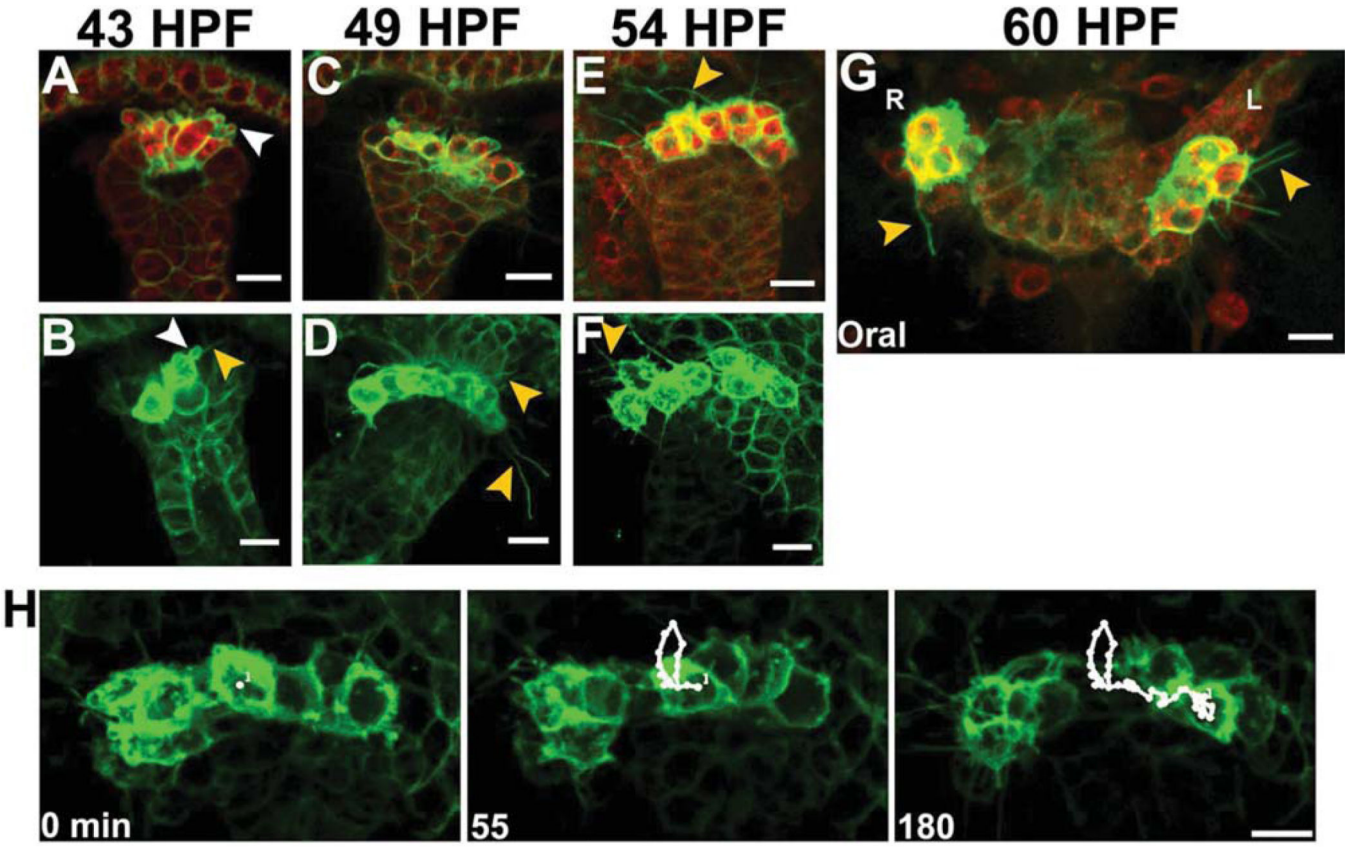

Fig. 6.

Small micromeres expressing PH-mCit develop cortical blebs (white arrowheads) and thin filopodia (orange arrowheads). Representative confocal snapshots of embryos containing small micromeres (**A, C, E**) expressing Vasa-mChr (red) and the PIP_2 marker, PH-mCit (green, **B, D, F**) or only PH-mCit, show small micromeres produce cortical blebs (A,B) at 43 HPF, and thin filopodia (C,F) between 49–54 HPF. Representative oral view (**G**) of coelomic pouches at 60 HPF indicates small micromeres produce filopodia after left/right segregation. **H:** Film strip of confocal time-lapse recording of small micromere expressing PH-mCit overlaid with results of cell tracking in white. Filmstrip shows a small micromere using filopodia to contact ectoderm before migrating to a coelomic pouch. Scale bars = 10 μm.

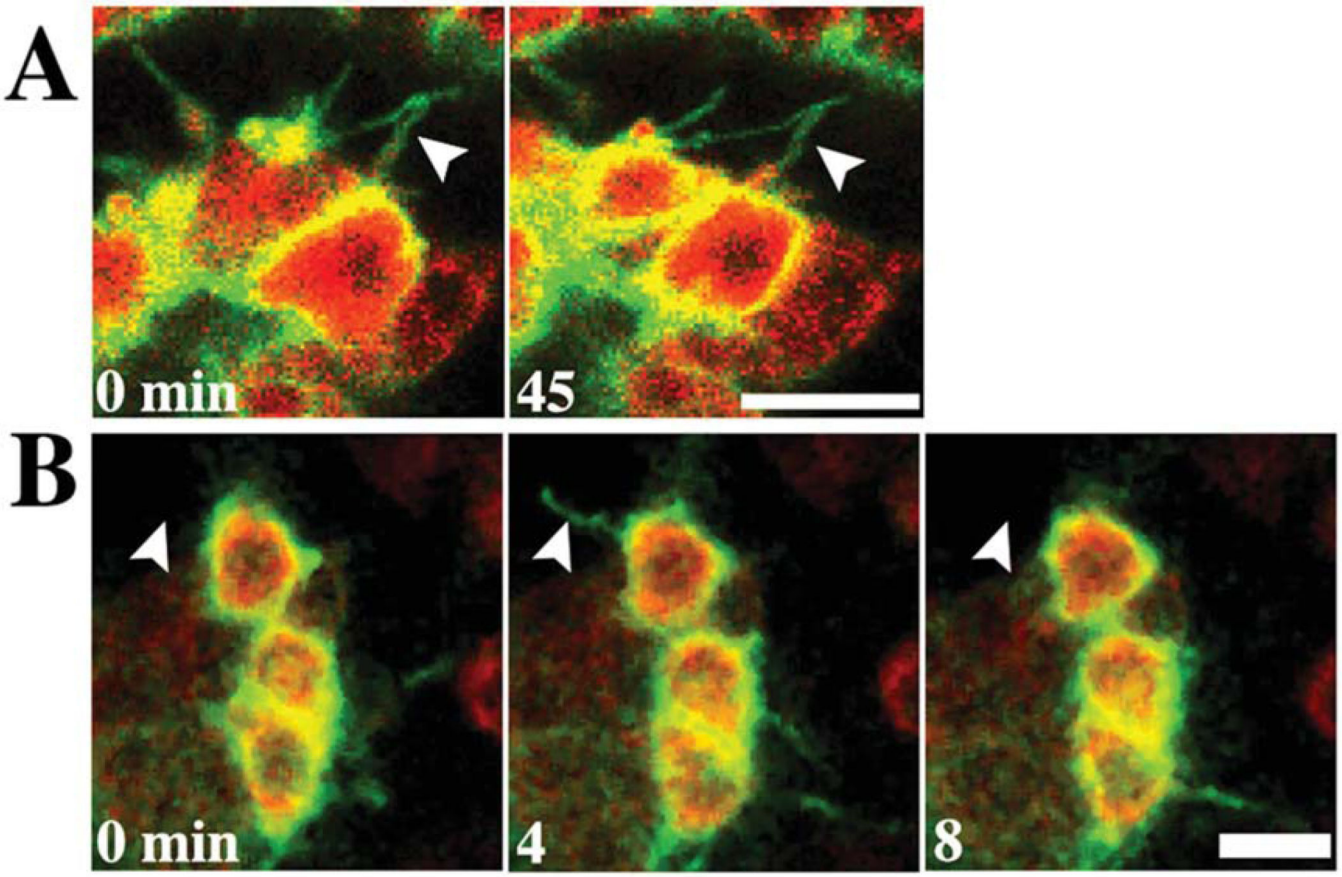

Fig. 7.

Small micromeres produce transient and stable filopodia. Confocal micrographs of representative small micromeres expressing Vasa-mChr (red) and PH-mCit (green) in coelomic pouches at 60 HPF that produce (**A**) stable filopodia that contact ectoderm for over 45 min and (**B**) short-lived filopodia that project into the blastocoel and last <10 min. Scale bars = 10 μm. White arrowheads indicate positions of filopodia.

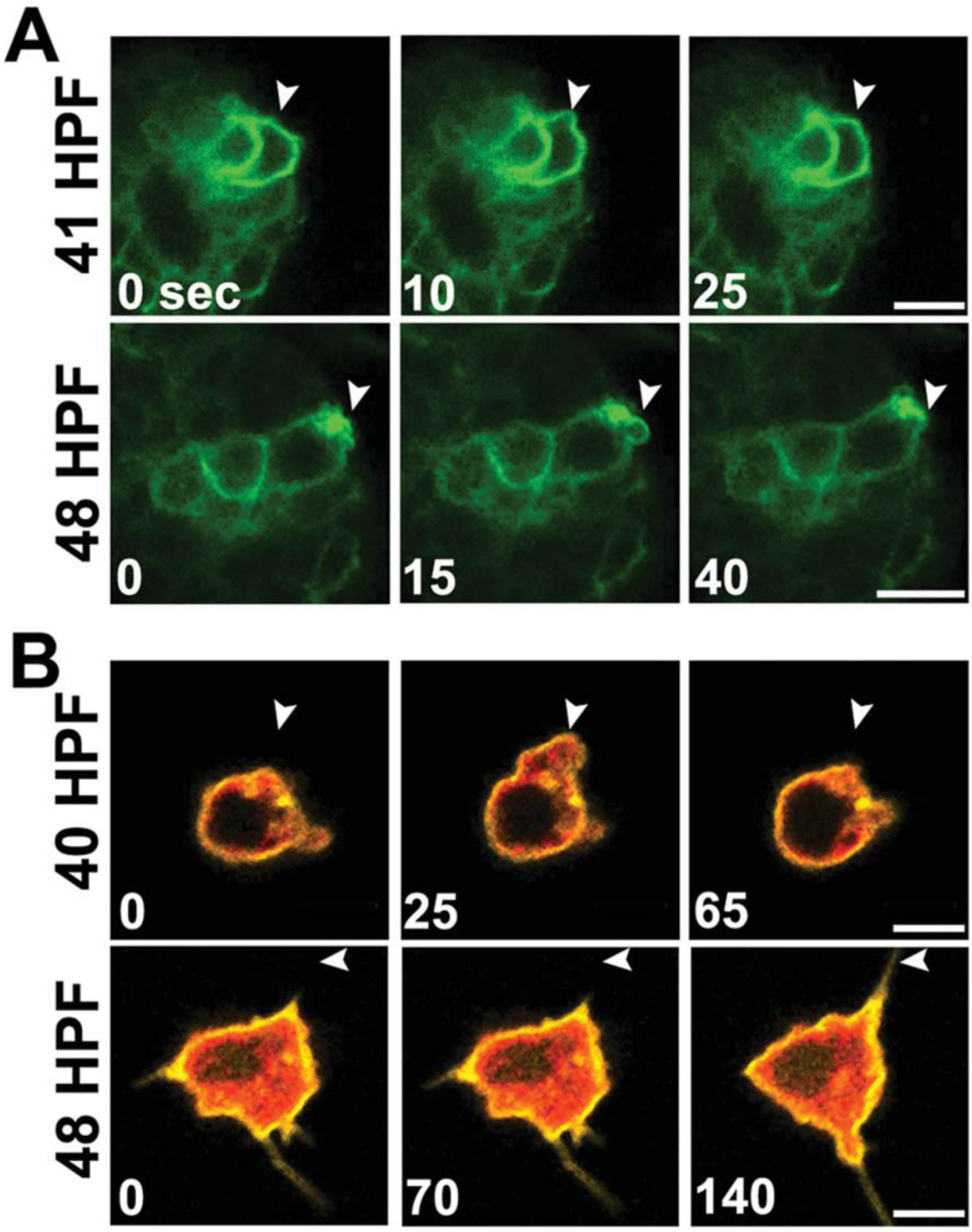

Fig. 8.

Small micromeres bleb rapidly in vivo and in vitro. **A:** Film strips of representative confocal time lapse recordings of small micromeres in vivo at 41 and 48 HPF expressing NTM-mCit (green) produce blebs (white arrowheads) that expand and contract within 1 min. **B:** Film strips of representative confocal time lapse recordings of small micromeres in vitro expressing NTM-mCit (yellow) and Vasa-mChr (red). White arrowheads at 40 HPF show the expansion and contraction of a cortical bleb within 1 min and at 48 HPF the extension of a filopodium in 140 sec. All scale bars = 10 μm.

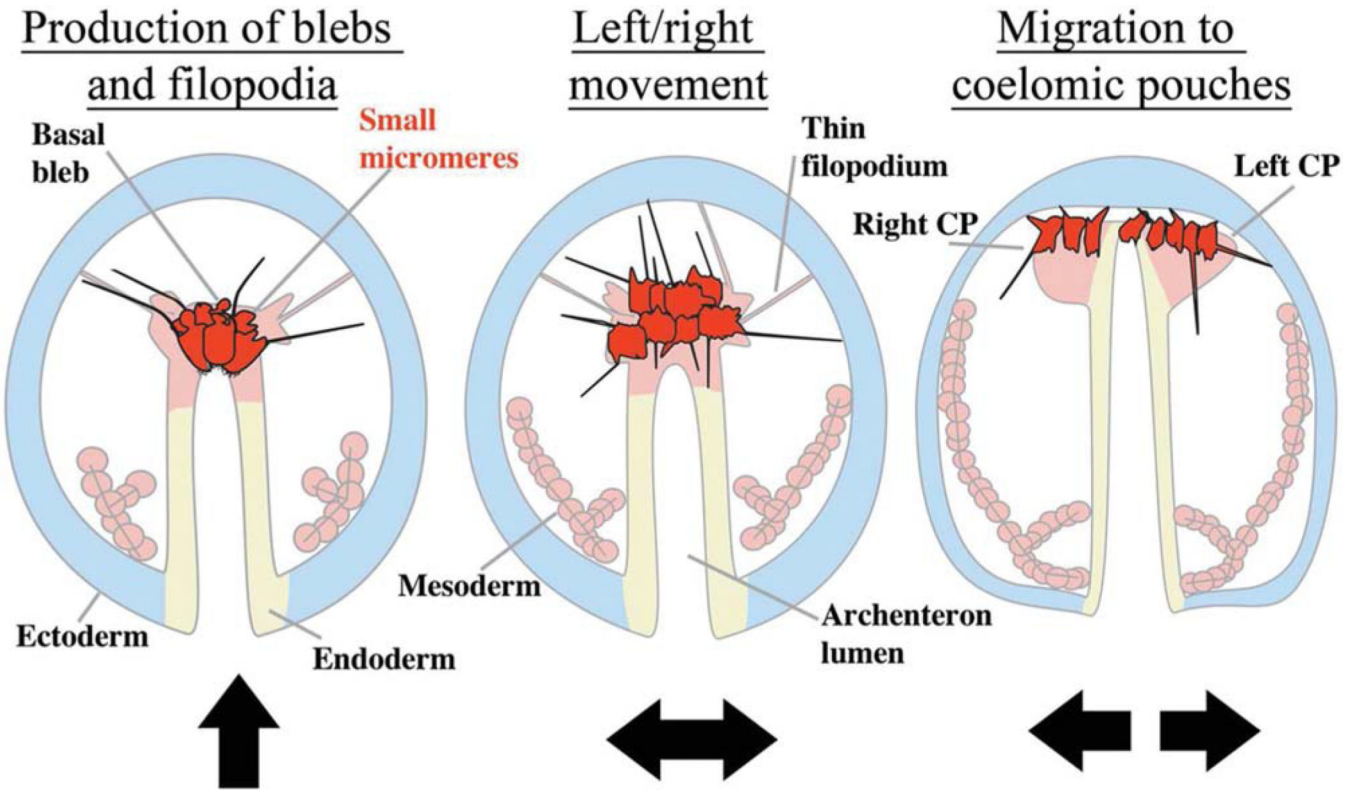

Fig. 9.

Schematic illustration depicting the phases of small micromere migration shown with arrows indicating the major direction of movement during each phase. During phase 1, small micromeres bleb basolaterally and produce filopodia to release from epithelium and move to the animal pole. In phase 2, small micromeres have taken a mesenchymal morphology, produce numerous filopodia and re-position along the left/right axis as they move to the roof of the archenteron. Phase 3 is characterized by the production of dynamic filopodia during the left/right segregation of small micromeres to the coelomic pouches.